# The Hydrodynamic Properties of Unsymmetrical Dual Vertical Slotted Walls

Hany G. I. Ahmed

*Associate professor of Irrigation and Hydraulics sector, Civil Engineering Dept, Al-Azhar University, Cairo, Egypt*, hanyahmed@azhar.edu.eg

Follow this and additional works at: https://mej.researchcommons.org/home

Mansoura University
Faculty of Engineering
Mansoura Engineering Journal

# The Hydrodynamic Properties of Unsymmetrical Dual Vertical Slotted Walls

Hany G. I. Ahmed*

*Abstract*— In terms of the importance of constructing mega coastal structures, in Egypt, hydrodynamic efficient economic measure should be innovated to protect such mega structures. Accordingly, this research was initiated with the objective of investigating an innovative hydrodynamic efficient economic breakwater, theoretically and numerically, where Unsymmetrical Dual Vertical Slotted-Walls "UDVSW" was proposed to be investigated. Primarily, literature in the field of breakwaters so as numerical models were assembled and scrutinized. A theoretical model was implemented and solved by Eigen-function technique for linear waves. In addition, a numerical model was constructed, where it is based on 3-D simulation code. The model investigated wavelength and wave period impact on UDVSW, in terms of its identities (i.e. solid length of its upper part and porosity of its lower part). Results were obtained; analyzed and presented. In addition, the numerical and theoretical results were compared against previous experimental results, from which clear their compatibility. The obtained results highlighted that the models are capable of estimating the energy dissipation, transmission and reflection coefficients within an acceptable accuracy, from the Engineering point of view. In addition, the results emphasized the efficient performance of the theoretical and numerical models in estimating UDVSW identities and wave velocity.

## I. INTRODUCTION

COASTAL regions are highly considered within the Egyptian development plan. Accordingly, there is a great attention towards protecting and sustaining beaches so as structures from being damaged by waves. This could be achieved by the available protection measures (i.e. breakwaters, groins and seawalls. However, some of them are not efficient or economic, while others fail to achieve their required protection. Such ineffectiveness emerges from their poor placement or from their design or from the improper selection of the protecting measure itself. Moreover, conventional breakwaters (i.e.rubble mound and gravity breakwaters) building material quantity increases as the depth

increases. In addition, they obstruct littoral drift causing imbalance of the sediment budget. Consequently, erosion and accretion occur in the neighboring beaches. Furthermore, they obstruct water circulation, which reduces the water quality within their vicinities. Additionally, they negatively affect the biodiversity. Accordingly, innovative breakwaters replaced the traditional ones. These novel types encompass double-permeable thin-walls, pre-cast dual vertical slotted-walls on piles. The slotted wall upper part is within the upper layer of the water and emerges above sea level, where the slotted part has closely spaced horizontal so as vertical slots. This type of breakwater reduces the pollution along coasts, as it allows a good water circulation.

***Corresponding Author:*** *Hany G. I. Ahmed, Associate professor at Irrigation and Hydraulics sector, Civil Engineering Dept, Al-Azhar University, Cairo, Egypt (e-mail: hanyahmed@azhar.edu.eg ).*

## II.    LITERATURE REVIEW

Researches in the field of breakwaters were assembled and scrutinized, from which clear was that little information about the proposed breakwater (i.e. UDVSW) was available. However, many experimental and theoretical studies were conducted. Moreover, numerical elaborations for wave interactions with UDVSW were presented by (Isaacson et al. 1999). They advocated that the porosity of the front wall and the ratio of incident wavelength to wave chamber width signify the reflection coefficient. Moreover, (Brossard et al. 2003) experimentally investigated the hydrodynamics of partially submerged wave-absorbing-breakwater. Likewise, (Suh, et al. 2007) put forward to theoretical methods to detect wave reflection away from perforated wall- piling- breakwater established due to potential flow. Similarly, laboratory tests were conducted for irregular waves and different chamber widths. Their study highlighted that the spectrum of the reflected wave has an oscillating activity dependent on frequency. Moreover, their results affirmed that reducing breakwater porosity enhances its characteristics. (Ji et al. 2016) probed four types of floating breakwaters. They asserted that the mesh cage is suitable for wave attenuation and has the least motion responses so as mooring forces, among the investigated types. (Elbisy et al. 2016) investigated hydrodynamic performance of breakwaters with many rows of vertical slots. They devised a mathematical technique based on Eigen-function and least-squares. They compared their results, in terms of reflection, transmission and dissipation coefficients, where the function $k_0h$ was utilized. They found out that the mathematical model designated the main identities of double- so as triple-row-breakwater. However, (Somervell et al. 2017) studied the hydrodynamics of vertical cellular breakwater with double barriers, while varying its upper and lower porosities. They utilized the Eigen-function approach, where they created a theoretical model for the hydrodynamic performance of cellular breakwater. Similarly, (Laju et al. 2007) investigated pile-supported, double-skirt breakwater, while (Ahmed et al. 2014), with the aid of theoretical and experimental models, examined dual-vertical-slotted-barriers wave-interaction. They established a numerical model (i.e. CFD) for regular wave interaction with these barriers. (Ahmed, et al. 2011) and (Elbisy, et al. 2016) established mathematical models, which were theoretically based on eigen-function technique for regular nonlinear wave-interactions with single, double and multiple-row slotted-breakwater. In addition, they utilized the Least- Square so as Eigen-function techniques and constructed a theoretical model.

On the other hand, few researchers dealt with comparable models, where no practical or theoretical investigation was held, in terms of horizontal-slots breakwater permeability performance. However, (Rageh and Koraim 2010) advocated that horizontal-bar-alignment induces higher wave attenuation so as resistance rather than vertical-bar-alignment. They proposed a theoretical model for designating the hydrodynamic performance of vertical-slotted-breakwater with impervious upper so as lower sections with porous middle section. They advocated that wave energy spreads equally across the depth. Consequently, a large portion of the wave energy passes via the slotted portion, where, as $k_h$ rises, the wave energy is concentrated at the still water level. Their findings affirmed that a properly constructed vertical-slotted-breakwater is nominated to be utilized in ports and shore protection (George and Cho 2020).

Based on the scrutinized literature, this study was originated with the impartial of utilizing theoretical so as numerical models to reconnoiter wave transmission-, reflection-, and energy dissipation-coefficients of UDVSW, where the impact of wave and physical properties on its hydrodynamic identities was examined. Among these identities were the impact of wavelength, wave period, solid length of the upper part, and porosity of the lower part. In addition, the study devised a theoretical model, based on Eigen-function approach, to investigate its hydrodynamic performance. On the other hand, the CFD numerical model is tooled to detect the velocity so as velocity vectors in the vicinity of the barrier.

## III.    THEORETICAL MODEL

The proposed breakwater is presented on figure 1, where $h$ represents the water depth; $2a$ exemplifies the distance between the centerlines of the barriers; $D_1$ and $D_2$ represent the draught of the upper part; $b_1$ and $b_2$ symbolize the wall thicknesses of the model, $w_1$ and $w_2$ signify the slot widths of the two lower parts, $H_i$, $H_r$ and $H_t$ represent the incident, reflected, and transmitted wave height, respectively and $c_1$ so as $c_2$ represent the slot gap-width. The coordinate system $(x, z)$ is located amid the pair of walls. The vertical-coordinate z is perpendicular to the water surface. The fluid domain was divided into zone 1, which is the seaward side of the breakwater, at x>-a. While zone 2, is the zone between the barriers, at -a≤x≤ a. On the other hand, zone 3 is the lee-side of the breakwater, at x>a.
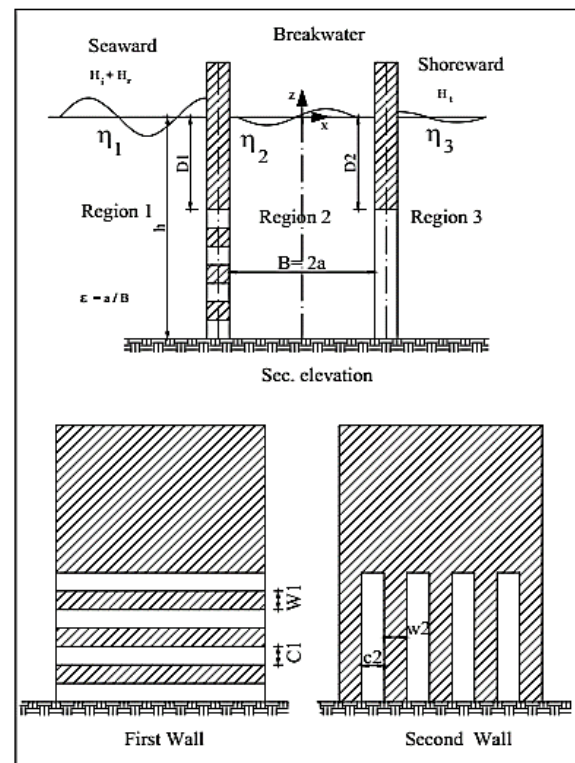


Fig. 1. Breakwater model schematic diagram.

*A. Boundary Value Problem*

*1. Velocity Potential*

Analysis was conducted on the basis of incompressible fluid and turbulent flow motion. Periodic motion, free surface and impermeable bottom boundary conditions were put forward to the model, where the velocity potential $[P_{(x-z-t)}]$ was calculated as follows, (Isaacson et al. 1999):

$$\varphi_{p_{(x,z,t)}} = Re[-\frac{igH_i}{2\omega}\frac{1}{cosh(kh)}\varphi_p(x,z)e^{-i\omega t}]$$
$$p = 1, 2, 3 \tag{1}$$

Where: $Re$ is the complex value of the real part, $i = \sqrt{-1}$, g is the acceleration due to gravity, $\omega$ symbolizes the frequency of angular wave ($\omega=2\pi/T$), $T$ is wave period, $k$ denotes wave number ($k=2\pi/L$), $L$ is wave length and $\phi = 1, 2, 3$ denotes the three wave-regions.

*2. Boundary Conditions*

The thickness of walls is assumed to approach zero. Accordingly, $\phi_{P(x, z)}$ ought to satisfy the boundary conditions, as follows:

$$\frac{\partial\varphi_p}{\partial z} = 0 \quad z = -h, \text{ (seabed-condition)}$$
$$p=1, 2, 3 \tag{2}$$

$$\frac{\partial\varphi_p}{\partial z} - \frac{\omega^2}{g}\varphi_p = 0$$
$$z = 0, \text{ (free-surface-condition)}$$
$$\phi = 1,2,3. \tag{3}$$

$$\underset{|x|\to\infty}{Lim}\left[\frac{\partial\varphi_p}{\partial|x|} - ik\varphi_p\right] = 0 \text{ (Radiation-condition)}$$
$$p=1, 3 \tag{4}$$

Walls boundary conditions:
At the impervious upper-parts:

$$\frac{\partial\varphi_1}{\partial x} = \frac{\partial\varphi_2}{\partial x} = 0, \quad x = -a, \quad 0 > z > -D1 \tag{5}$$

$$\frac{\partial\varphi_2}{\partial x} = \frac{\partial\varphi_3}{\partial x} = 0, \quad x = a, \quad 0 > z > -D2 \tag{6}$$

At the pervious lower-parts
$$\frac{\partial\varphi_1}{\partial x} = \frac{\partial\varphi_2}{\partial x} = -iG_1{}^\backslash(\varphi_2 - \varphi_1),$$
$$x = -a, \quad -D1 > z > -h \tag{7}$$

$$\frac{\partial\varphi_2}{\partial x} = \frac{\partial\varphi_3}{\partial x} = -iG_2{}^\backslash(\varphi_3 - \varphi_2)$$
$$, x = a, \quad -D2 > z > -h \tag{8}$$

According to Eq. (5) and Eq. (6), the horizontal velocities diminish. Eq. (7) and Eq. (8) describe that horizontal velocities is equal at breakwater edges, for the two regions. The permeability factors were explained by (Sollitt and Cross 1972), and (Isaacson, et al. 1998), as follows:
$$G = \varepsilon / (f - is), \tag{9}$$

In which, $\varepsilon$ is porosity ($\varepsilon=c/(c+w)$), $f$ denotes friction coefficient, which is implicitly calculated by equivalent work of Lorentz principle. It was considered constant for both walls, while $s$ symbolizes inertia-coefficient:

$$s = 1 + cm(\frac{1-\varepsilon}{\varepsilon}), \tag{10}$$

Where: $cm$ is added-mass-coefficient and is taken as a constant that approaches zero (Isaacson et al. 1999).

*B. Flow Potential Solution*

In order to designate $\phi_1$, $\phi_2$, and $\phi_3$ that satisfy the seabed-, free-surface-, and radiation-conditions, Eigen-function technique is used to solve the equations (Laju, et al.), where the velocity potentials are presented by using a the following solutions:

$$\varphi_1(x,z) = \varphi_I + \sum_{n=0}^{\infty} A_{1n} \cos\mu_n (z+h)e^{\mu_n(x+a)},$$
$$x \leq -a \tag{11}$$

$$\phi_2(x,z) = \sum_{n=0}^{\infty} A_{2n}\cos\mu_n(z+h)e^{-\mu_n(x+a)} +$$
$$\sum_{n=0}^{\infty} A_{3n}\cos\mu_n(z+h)e^{\mu_n(x-a)},$$
$$-a \leq x \leq a \tag{12}$$

$$\varphi_3(x,z) = \sum_{n=0}^{\infty} A_{4n}\cos\mu_n(z+h)e^{-\mu_n(x-a)}, x \geq a \tag{13}$$

Where: $\phi_I$ signifies incident wave potential, which is given as:
$$\varphi_I(x,z) = \cosh k (z+h)e^{ikx} \tag{14}$$

Moreover, $\mu_n$, for $n \geq 1$ of non-propagating diminishing waves:
$$\omega^2 = -g\mu_n \tan(\mu_n h) \quad \text{For } n \geq 1 \tag{15}$$

The number $\mu_o$ is the imaginary root of the propagating waves equation, such that $\mu_o = -ik$:
$$\omega^2 = -gk \tanh(kh) \quad \text{For } n = 0 \tag{16}$$

*C. Reflection-, Transmission-, And Energy Dissipation-Coefficients*

The theoretical reflection- and transmission-coefficients ($K_r$ and $K_t$) were determined after solving boundary condition and governing equations (i.e. $A_{10}$ and $A_{40}$) and are evaluated as follows:

$$K_t = |A_{40}| \tag{17}$$
$$K_r = |A_{10}| \tag{18}$$

Theoretically, the energy losses of the incident wave are given as: $E_i = E_r + E_t$ (19)
Where, $E_r$, $E_t$ and $E_i$ symbolize the reflected-, transmitted- and incident-wave energies, respectively. Accordingly, Eq. (43) is rephrased as follows:

$$K_r{}^2 + K_t{}^2 = 1 \tag{20}$$

When the wave encounters the structure, portion of wave-energy is dissipated by it. This ration of energy is calculated after (Isaacson et al. 1999) reflectivity coefficients:

$$K_d = \sqrt{1 - K_r{}^2 - K_t{}^2} \qquad (21)$$

Where: $K_d$ denotes wave-energy dissipation-coefficient.

## IV. NUMERICAL MODEL

This section presents the implemented CFD model and its theory. The section describes the model validation and its numerical simulations of the proposed UDVSW breakwater. The FLOW-3D code examines its hydraulic performance, whereas its mass, energy conservation and momentum equation were utilized. The finite difference method was tooled to solve the equations. The numerical algorithm is called **S**olution **A**lgorithm-**V**olume of **F**luid "SOLA-VOF", (Flow Science 2011.

### A. Implemented Model

The proposed UDVSW breakwater was investigated by tooling the commercial Computational Fluid Dynamics package of FLOW-3D. This package was selected to be tooled, as it was apparent from the literature that it is applicable in many engineering practices, especially in Marine- and Coastal-Engineering applications.

### B. Theory of CFD Code

CFD code (i.e. Flow-3D) solves 3-D Reynolds Averaged Navier Stokes "RANS" equations by finite-volume-theory. The model encompasses many solid sub-components; figure (2). FLOW-3D reflects the geometrical so as hydraulic boundary conditions. In order to obtain reasonable accuracy, the mesh cell was taken as 1 x 1 cm, for all frequencies.
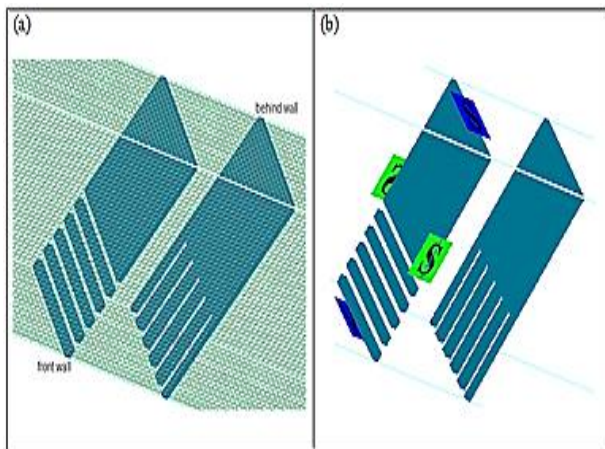


Fig. 2. Proposed Breakwater Model in flow-3D (a) meshing geometry and (b) boundary condition

## V. RESULT ANALYSIS AND VERIFICATION

### A. Validation the Theoretical and Numerical Models

Due to the unavailability of experimental results for UDVSW, theoretical and numerical models, for one-wall with horizontal slots, in the lower part, was developed and compared

to previous experimental results (Rageh and Koraim 2010). The comparison is presented on figure 3, for a similar case with similar characteristics and conditions. Their experiment work was carried out in a 15 m long, 1 m deep and 1m wide wave flume. The water depth was 0.5 m. Their model was built from wood with 0.02 m horizontal slots and a thickness of 0.025m. The upper draft $D_1$ was 0.36 $h$ and the porosity was 0.5. Regular wave trains period $T$ ranged between 0.9 to 1.9 s. The obtained results were compatible to (Rageh and Koraim 2010), where the present theoretical and numerical with one barrier has a friction factor $f$ of 3.5.

Figure 4 shows the results of the present theoretical study for the reflection- and transmission-coefficients compared to previous experimental results of (Rageh and Koraim 2010) and the present numerical study. Noticeable was the slight discrepancies of the theoretical and numerical results. Apparent was also that for most of the experiments, such divergences ranged between + 5% and -5%, where only few points indicated a range between more than +5% and less than – 10%. This result was within the acceptable range of the Engineering practice. Confident with these results, the present model was validated against similar characteristics to detect the UDVSW hydrodynamic properties.
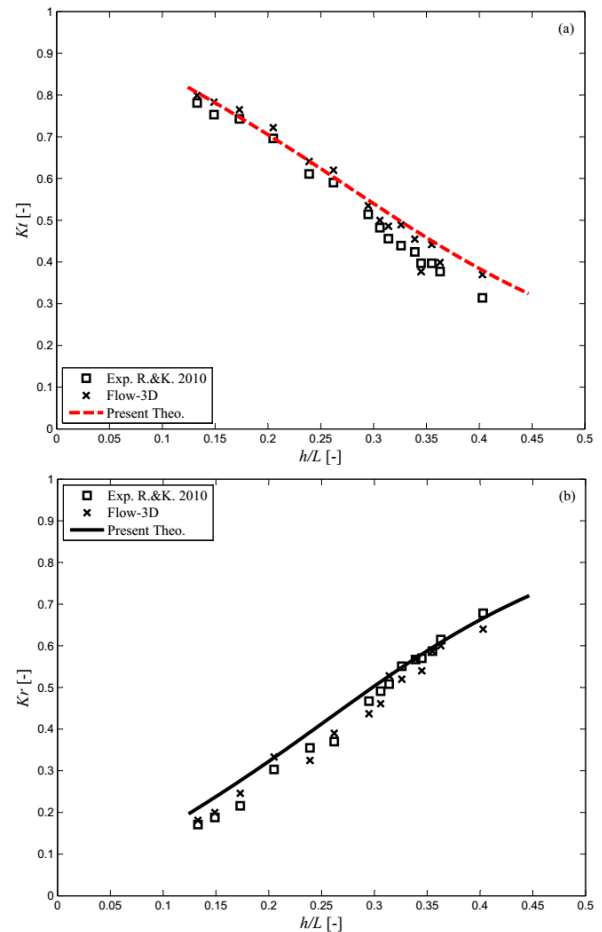


Fig. 3. CFD (FLOW-3D) results versus theoretical results as function of (h/L), at B/h=0.5, D/h=0.5 and ε =0.5 (a) $K_t$, and (b) $K_r$
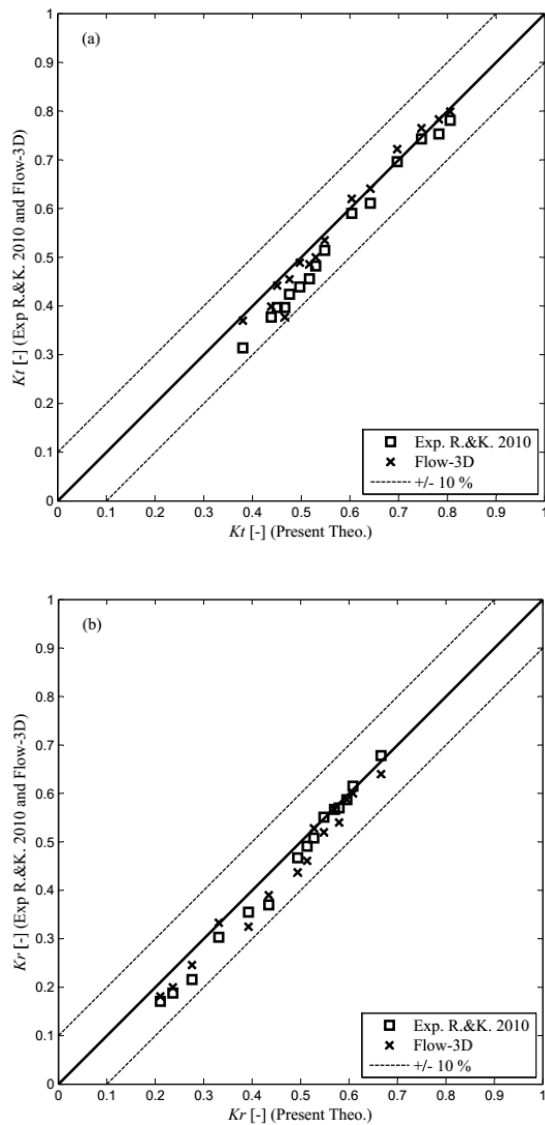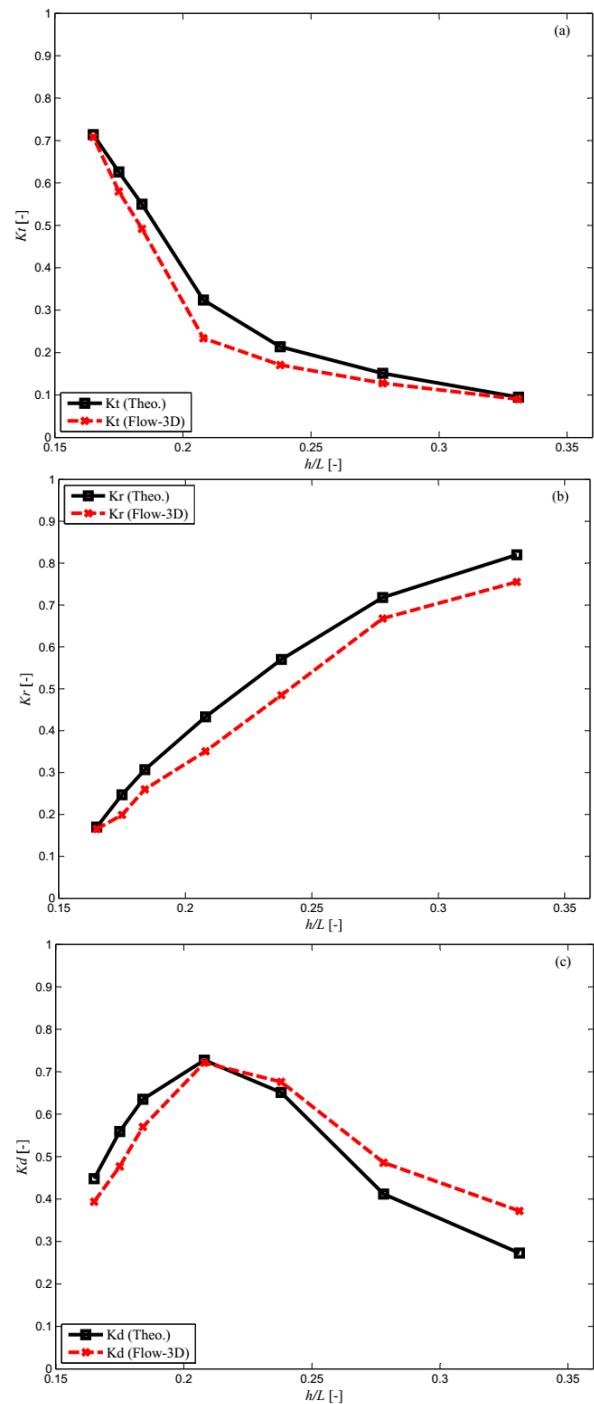
Fig. 4.  CFD (FLOW-3D) results versus theoretical results
as a function of (h/L), at B/h=0.5, D/h=0.5 and ε =0.5
(a) $K_t$, and  (b) K.

## B. The Hydrodynamic Properties of the Present Models

It should be noted that UDVSW performance, in terms of reflection-, transmission-, and dissipated-energy was studied theoretically, and numerically; figure 5. The theoretical results indicated the same trend as the numerical model results, when the friction factor $f$ was 3.5. In addition, they provided reasonable estimates for energy dissipation coefficient. Confident with the results, the reflection-coefficient "$K_r$" increased, as h/L increased, at a fixed D of 0.5 h. In contrast, the transmission-coefficient "$K_t$" indicated an opposite trend. These results indicated that the proposed UDVSW plays a significant role in decreasing the transition-coefficient and increasing the energy dissipation-coefficient. As an example, the transmitted wave decreased by 30% and the dissipated energy increased by more than 70%, at h/L = 0.21.



Fig. 5.  CFD (FLOW-3D) results versus theoretical results
as function of (h/L), at B/h=0.5, D/h=0.5 and ε =0.5
(a) $K_t$,   (b) $K_r$  and  (c) $K_d$

## C. Study the Effect of Draught "D" and Chamber Width "B" on Hydrodynamics Coefficients

The impact of the relative chamber width "$B/h$" on the $K_t$, $K_r$, and $K_d$ is elaborated on figure 6, from which clear was that at $D/h$ =0.5, $B/h$=0.5, 1.0 and 1.5, $K_t$ decreases as $h/L$ increases. In addition, the figure indicates that $B/h$ is of tangible significance, while the impact on $K_r$ is unlike that of $K_t$. On the other hand, figure 7 explains the relative upper part draught "$D/h$" impact on $K_t$, $K_r$ and $K_d$, where similar trends of $K_t$, $K_r$ and $K_d$ to the impact

of relative chamber width. Noticeable was also the impact of "D/h" on the hydrodynamic-coefficients.
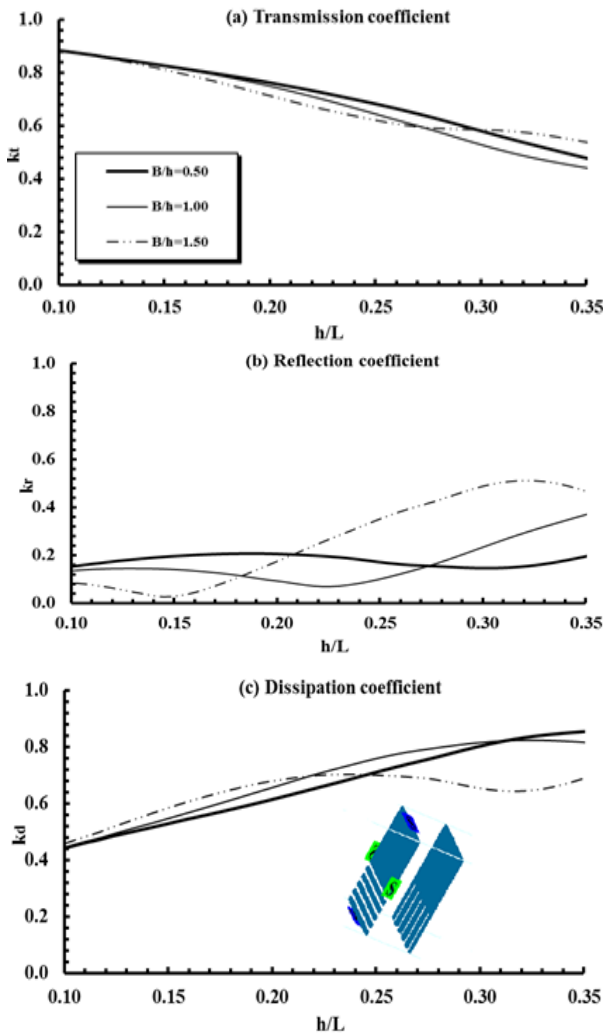


Fig. 6. Impact of B/h on hydrodynamic coefficients by FLOW-3D
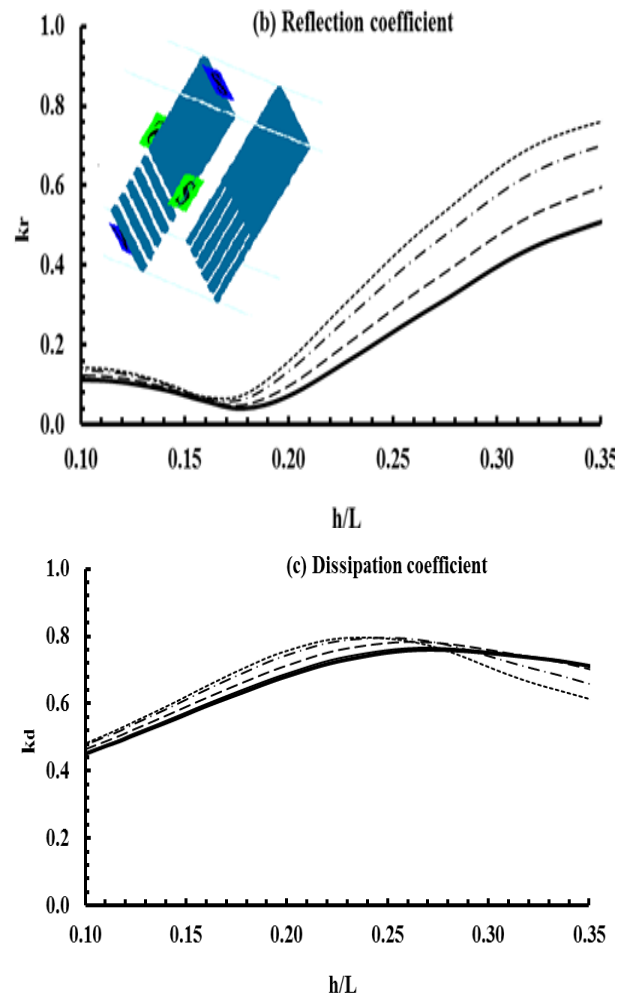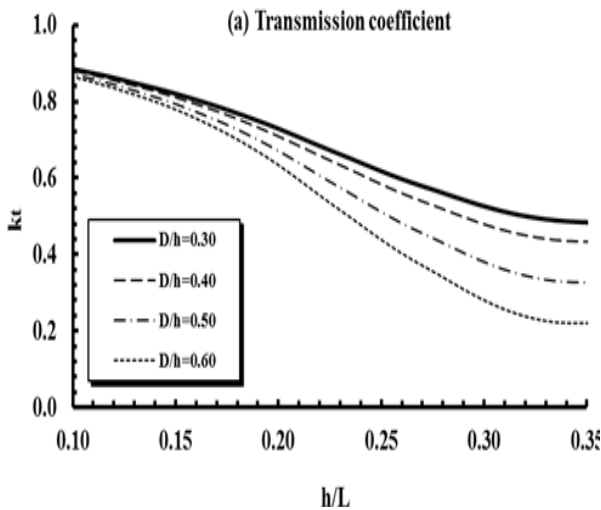At  *D/h* =0.5, *D/h*=0.5  (a) $K_t$, (b) $K_r$ and (c) $K_d$.





Fig. 7. Impact of D/h on the hydrodynamic coefficients by FLOW-3D
At  $K_d$=0.5, *B/h*=0.5 (a) $K_t$, (b) $K_r$ and (c) $K_d$

## D. Velocity and Pressure Distribution

Numerical and theoretical simulations, of UDVSW breakwater, were compared, where a satisfactory agreement was evident. Accordingly, the velocity and pressure distribution in UDVSW vicinity was provided. The numerical model was tooled to identify velocity field and vectors, in UDVSW vicinity. This was achieved to suggest a strategy for wave energy dissipation.

### 1.  Velocity Distribution

FLOW-3D provided a plotting to both velocity-vector and velocity-field, for one cycle at an interval of 0.1 sec, at a wave period of 1.10 sec; figure 8. Greater velocities are evident near the wave peak and around slots. Greater velocities are induced at slots due to the barrier impact. On the other hand, the velocity-magnitude is very high in front of and behind the barrier. This is attributed to the fact that some of the wave energy is halted and another part is transferred, while the rest is lost in a vortex. The transmitted portion is redistributed over the depth. This occurs at a distance equals to the water depth. The area around the barrier is denoted as Flow-3D, whereas the remainder is

signified as 2-D flow. The flow is turbulent in-between the barriers, while the motion is vertical except near slots.
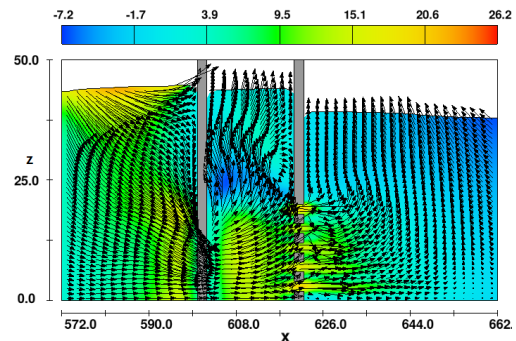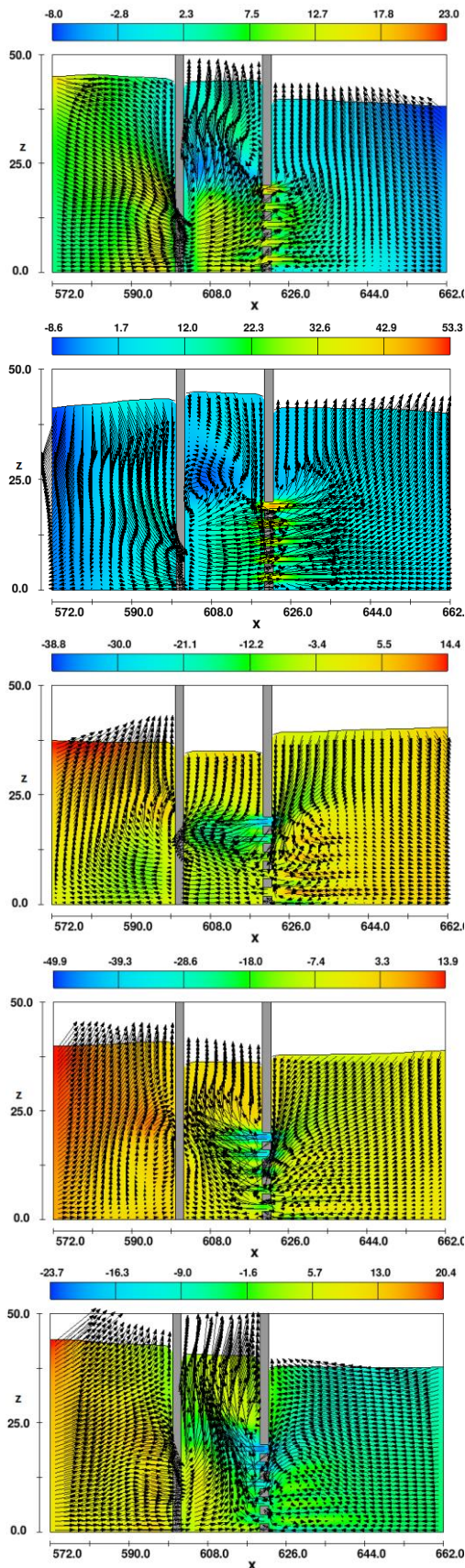




Fig. 8. FLOW-3D velocity (*cm/s*) and velocity-vector of UDSVW at= (10:11) sec for
$T$=1.1 sec, $h_i$ = 10 cm, $dt$ = 0.1 sec and $B/h$=0.5

## 2. Velocity Measurement

The maximum velocity was measured. During a cycle of waves, the measured velocity was 60.1 cm/s, in the vicinity of the impermeable barriers; figure (9), where the figure depicts that water mass interaction with holes on the barriers. From the figure, clear was the numerical model capability to predict the velocity-magnitude and velocity-vector within reasonable accuracy.
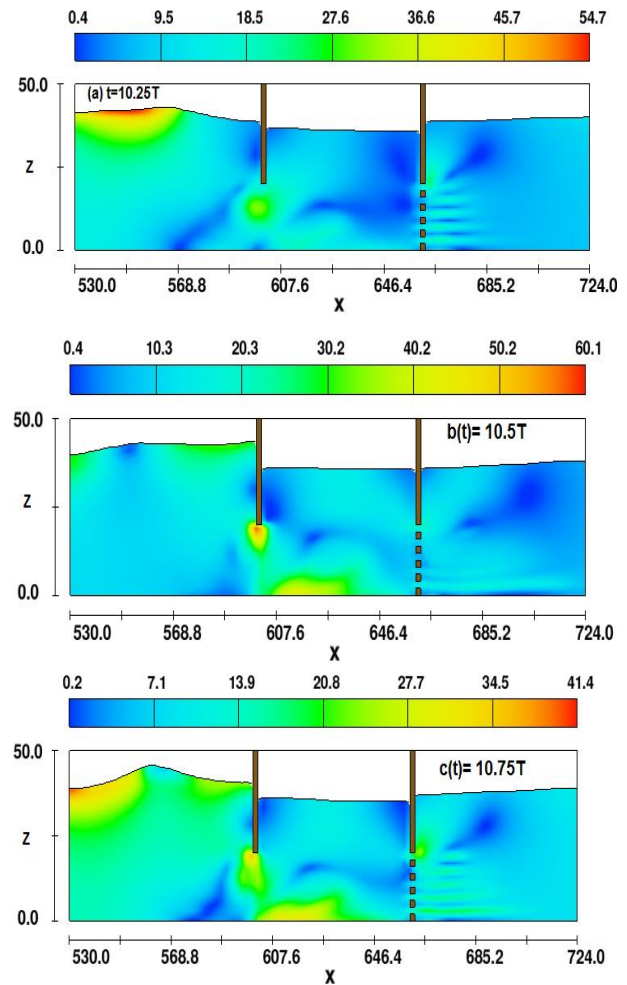


Fig.9. Velocity field in the vicinity of the barrier
At ☐ is 0.50, $B/h$ = 1.0 and $h_i$ = 9 cm, $T$=1.20 sec
a) $t$=10.25$T$   b) t=10.5$T$, and c) $t$=10.75$T$.

# VI.CONCLUSIONS

Within the framework of constructing massive coastal structures, in Egypt, an efficient economic structure should be innovated to protect such massive structures. Accordingly, this research was originated with the impartial of investigating an efficient economic UDVSW breakwater, theoretically and numerically. A theoretical model based on Eigen-function technique for linear waves was implemented. In addition, a numerical model was established. It is based on 3-D CFD code. The model investigated the wave period and wave length influence on UDVSW, in terms of its characteristics (i.e. solid upper part length and lower part porosity). The numerical and theoretical results were compared to previous experimental results, from which the following conclusions were deduced:

- Due to the unavailability of experimental results for UDVSW, the numerical and theoretical results of one barrier were compared to the results of previous experimental work of (Rageh and Koraim 2010), where a reasonable agreement was evident for similar characteristics and conditions.
- The results affirmed that the models are apt of providing energy dissipation-, transmission- and reflection-coefficients, within reasonable accuracy.
- The results underlined the effective capabilities of the theoretical and numerical models in identifying UDVSW characteristics.
- The results of the theoretical model and the numerical model indicated similar trends at a friction factor f=3.5. In addition, they portrayed reasonable estimation of transmission-, reflection-, and energy dissipation-coefficients.
- The impact of the relative chamber width (B/h) and the relative depth of solid upper part D/h on the hydrodynamic coefficients (kt, kr, and kd) was significant.
- The numerical model, based on Flow-3D technique, and the theoretical model indicated discrepancies in hydrodynamic parameters, wave-velocity and wave-magnitude.

## DECLARATION OF CONFLICTING INTERESTS STATEMENT:

The author affirms that there is no potential-conflict of interest, in terms of research author-ship or publication.

# REFERENCES

[1] A. George, and H. Cho, 2020. "Hydrodynamic Performance of a Vertical Slotted Breakwater," International Journal of Naval Architecture and Ocean Engineering 12: 468–78.

[2] C. Ji, X. Chen, J. Cui, O. Gaidai, and A. Incecik, 2016. "Experimental Study on Configuration Optimization of Floating Breakwaters," Ocean Engineering 117: 302–10.

[3] C.K. Sollitt, and R.H. Cross, 1972. "Wave Transmission through Permeable Breakwaters," Proceedings of the 13th Coastal Eng. Conf., ASCE, Vancouver: 1827–46.

[4] Flow Science. 2011. "FLOW-3D V9.4 User's Manuals,": 3–4.

[5] H. Ahmed, and A. Schlenkhoff, 2014. "Numerical Investigation of Wave Interaction with Double Vertical Slotted Walls," Engineering and Technology International Journal of Environmental, Ecological, Geological and Mining Engineering 8(8): 1447–55.

[6] H. Ahmed, A. Schlenkhoff, and M. Oertel, 2011. "Stokes Second-Order Wave Interaction with Vertical Slotted Wall Breakwater," Coastal Structures Conference, Yokohama, Japan: 691–703.

[7] Isaacson, M., J. Baldwim, S. Premasiro, and G. Yang. 1999. "Wave Interaction with Double Slotted Barriers," Applied Ocean Research 21: 81–91.

[8] J. Brossard, A. Jarno-Druaux, F. Marin, and E.H. Tabet-Aoul. 2003. "Fixed Absorbing Semi-Immersed Breakwater," Coastal Engineering 49: 25–41.

[9] K. Laju, V. Sundar, and R. Sundaravadivelu. 2007. "Studies on Pile Supported Double Skirt Breakwater Models," Journal of Ocean Technology 2(1): 32–53.

[10] K.D. Suh, H. Y. Jung, and C.K. Pyun, 2007. "Wave Reflection and Transmission by Curtain Wall–Pile Breakwaters Using Circular Piles," Ocean Engineering 34: 2100–2106.

[11] L. Somervell, S.G. Thampi, and A.P. Shashikala, 2017. "Hydrodynamic Characteristics of Vertical Cellular Breakwater," Waterway. Port, Coast. Ocean Eng. 143(5).

[12] M.S. Elbisy, E.M. Mlybari, and M.M. Helal, 2016. "Hydrodynamic Performance of Multiple-Row Slotted Breakwaters," Journal of Marine Science and Application 15(2): 123–35.

[13] M. Isaacson, S. Premasiro, and G. Yang. 1998. "Wave Interaction with Vertical Slotted Barrier," Journal Waterway, Port, Coastal and Ocean Eng. 124(3): 118–26.

[14] O.S. Rageh and A.S. Koraim, 2010. "Hydraulic Performance of Vertical Walls with Horizontal Slots Used as Breakwater," Coastal Engineering 57(8): 745–756.

**Arabic Title:**

الخصائص الهيدروديناميكية للحواجز المشقوقة العمودية المزدوجة
غير المتماثلة

**Arabic Abstract:**

نظرا لأهمية بناء المنشآت الساحلية الضخمة، في مصر، فهناك ضروره لابتكار تدابير اقتصادية هيدروديناميكية فعالة لحماية مثل هذه المنشآت الضخمة. فهذا البحث يهدف الى التحقق من حاجز أمواج اقتصادي مبتكر ذو كفاءة هيدروديناميكية عالية، نظريًا وعدديًا. وبناء عليه، تم اقتراح ودراسة صفين من حواجز الأمواج العمودية الغير متماثلة "UDVSW". ففي المقام الأول ، تم تجميع وفحص الدراسات السابقة في مجال حواجز الأمواج والنماذج العددية. كما تم استحداث نموذج نظري بتقنية دالة Eigen للموجات الخطية. بالإضافة إلى ذلك ، تم إنشاء نموذج رقمي، حيث يعتمد على محاكاة ثلاثية الأبعاد. وتم دراسة تأثير طول الموجة وزمنها على المقترح UDVSW، من حيث الطول الصلب للجزء العلوي ومسامية الجزء السفلي منه. وتم الحصول على نتائج ؛ وتم تحليلها وعرضها. بالإضافة إلى ذلك، تمت مقارنة النتائج العددية والنظرية بالنتائج التجريبية السابقة والتي من خلالها تم التأكد من توافقها. وأوضحت النتائج المتحصل عليها أن النماذج قادرة على تقدير معاملات تبديد الطاقة والانتقال والانعكاس بدقة مقبولة هندسيا. بالإضافة إلى ذلك ، أكدت النتائج على كفاءة أداء النموذج النظرى والعددى في تقدير خصائص UDVSW وسرعة الموجة، بشكل مثالي.